Engineering Structures 217 (2020) 110557

Contents lists available at ScienceDirect

Engineering Structures

journal homepage: www.elsevier.com/locate/engstruct

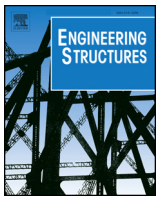

New design model for brittle failure in the parallel-to-grain direction of timber connections with large diameter fasteners

Miguel Yurrita*, José Manuel Cabrero

Wood Chair, Department of Building Construction, Services and Structures, University of Navarra, 31009 Pamplona, Spain

ARTICLE INFO

Keywords:
Timber connection
Brittle failure
Parallel-to-grain
Dowel-type fastener
Eurocode 5

ABSTRACT

Timber connections may collapse in a brittle or in a ductile mode. The calculation models of timber joints are mainly focused on ductile failure mode, since it has been traditionally assumed that brittle failure was avoided by respecting a minimum spacing between fasteners. However, this assumption alone does not guarantee a ductile failure. This paper proposes a new design model dealing with brittle failure modes of timber connections with large diameter fasteners (those protruding the whole thickness of the timber member such as dowels or bolts). A comparison between the proposal and the existing models, using an extensive database of tests, is used to demonstrate the improved accuracy of the proposed design method.

1. Introduction

Environmental awareness, combined with politics that encourage the use of sustainable and renewable materials, clearly influence the building sector. The increased use of timber structures during the last years is thus expected to continue in the future.

Connections have a main role in the structural design, as they highly influence the behaviour, cost, and safety of structures. Connections were related with around 25% of recent collapses of timber structures, and around half of these cases involved connections with dowel-type fasteners [1,2].

A connection with dowel-type fasteners may fail in a ductile or a brittle manner. The European Yield Model (EYM), which is worldwide used to determine the capacity of a connection, considers only the ductile failure mode, namely embedment (Fig. 1a) and yielding of the fastener.

However, a timber connection may prematurely fail before achieving such ductile capacity, at a lower load, in a brittle manner: splitting (Fig. 1b), row shear (Fig. 1c), block shear (Fig. 1d) or net tension (Fig. 1e). Such early brittle failure may lead not only to a reduction of the intended capacity but, in a poorly designed building lacking robustness, to a possible sudden collapse of the building. However, as important as it may be, it is quite an unknown topic. As demonstrated by a survey made by the Working Group 3 of the Cost Action FP1402 [3], 30% of the participants (most of them European) ignored the existence of such kind of failure in connections.

Since reported in early works such as Fahlbusch [4], several authors have dealt with some or all of the possible brittle failure modes. For a detailed review, the reader is referred to Cabrero and Yurrita [5,6]. In the last 15 years, some of these models dealing with brittle failure have been included to a different extent in design standards, such as the Eurocode 5 [7], CSA Standard O86-09 [8] or the evolution of the latter one made by Quenneville and Zarnani [9] which will be included in the future chapter of the New Zealand standard dealing with connections.

This article presents a new design model for brittle failure of timber connections loaded in the parallel-to-grain direction with large diameter fasteners (such as dowels and bolts -defined in the Eurocode 5 [7] as the ones with a diameter larger than 6 mm- and which, by its configuration, usually protrude the whole timber thickness). The new model enables to calculate the brittle capacity of this kind of connections in a simple way, with an improved accuracy in comparison to the existing models.

This paper is organised as follows: Section 2 provides a brief description of the analysed type of structural connections, their brittle failure modes and existing models. Section 3 discusses the different assumptions and improvements of the new model in comparison to previous proposals. The full model is described in Section 4. Finally, in Section 5, an extensive data of experimental results is used to validate the new design model and compare its results with those obtained from other proposals.

* Corresponding author.
E-mail addresses: myurrital@alumni.unav.es (M. Yurrita), jcabrero@unav.es (J.M. Cabrero).

https://doi.org/10.1016/j.engstruct.2020.110557
Received 28 September 2019; Received in revised form 6 March 2020; Accepted 20 March 2020
Available online 26 May 2020

Nomenclature

Lower case

a_1	Spacing between columns of fasteners
a_2	Spacing between rows of fasteners
a_3	Distance between the last column of fasteners and the the loaded edge of the timber element
a_4	Distance between the side row of fasteners and the edge of the timber element
b	Width of a timber member
b_c,b_{net}	Width between the two lateral row of fasteners (gross and net distance, respectively
c	Rank correlation coefficient [42]
d	Fastener diameter
d_0	Diameter of the pre-drilled hole for a fastener
f_u	Ultimate strength of the fastener
f_v	Shear strength of a timber product
$f_{h,0}$	Embedment strength in the parallel-to-grain direction
$f_{t,0}$	Tensile strength in the parallel-to-grain direction of a timber product
k_t	Coefficient applied to the head tensile plane
k_v	Coefficient applied to the lateral shear planes
m	Slope of a linear fit passing through the origin of co-ordinates
n_c	Number of columns of fasteners
n_{ef}	Effective number of fasteners
n_r	Number of rows of fasteners
n_s	Number of shear planes of a connection
sws	Steel-wood-steel connection
t	Thickness of the wood member
t_1, t_2	Thickness of the side and middle timber member, rspectively
t_{ef}	Effective thickness of the connection
t_p	Steel plate thickness
msp	Multiple shear plane connection
ws	Wood-steel connection
wsw	Wood-steel-wood connection
ww	Wood-wood connection
www	Wood-wood-wood connection

Upper case

$A_{T,b}$, $A_{T,n}$	Head tensile area related to block shear and net tension, respectively
BOEF	Beam on elastic foundation
CCC	Concordance correlation coefficient [43,41,44]
COV	Coefficient of variation
EYM	European Yield Model
F_B	Brittle load capacity of a connection
F_p	Theoretical load capacity of a connection predicted by a model
F_t	Load capacity of a connection experimentally tested
$F_{b,bs,i}$	Brittle load capacity of a timber element for block shear
$F_{b,i}$	Brittle load capacity of a connection
$F_{b,i}$	Brittle load capacity of a timber element
$F_{b,nt,i}$	Brittle load capacity of a timber element for net tension
$F_{b,rs,i}$	Brittle load capacity of a timber element for row shear
$F_{L,i}$	Load capacity of a single lateral shear plane
$F_{T,i}$	Load capacity of the head tensile plane
$F_{T,net,i}$	Load capacity of the head tensile plane for net tension
L_c, L_{net}	Length of the connection. Gross and net length, respectively
M_y	Yield moment of the fastener
MRE	Mean relative error
Q^2	Coefficient of correlation [40,41]
R^2	Coefficient of determination
SD	Standard deviation of the mean relative error

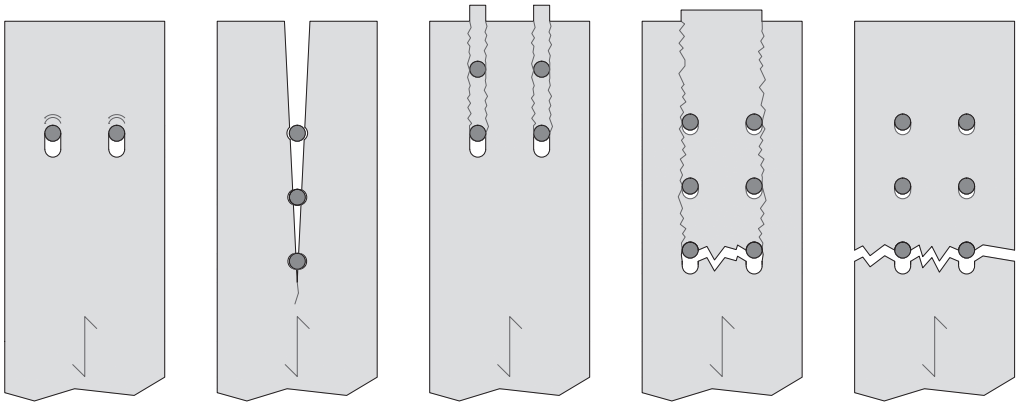

Fig. 1. Possible failure modes of a timber connection with dowel-type fasteners: embedment is the only ductile failure mode, the rest are brittle.

2. State of the art

2.1. Geometry of the connection

Fig. 2 shows a typical configuration of a timber-to-steel connection (in this case a wood-steel-wood, *wsw*, joint with two shear planes) with large diameter fasteners, (in this case, dowels). The timber elements are defined by its main dimensions: width b and thickness t_1 (t_2 for inner timber members in multiple shear plane connections, *msp*); the joint by its width b_c and length L_c, and the steel plates by its thickness t_p.

The connection depicted in Fig. 2 has a total of 12 fasteners with a diameter d, which fit in pre-drilled holes of diameter d_0 (which, in the case of bolts are oversized, $d_0 = d + 2$ mm), distributed in 3 rows in the parallel direction (n_r) and 4 columns (n_c) in the perpendicular to grain direction. The spacing between columns is defined as a_1;a_2 is the distance between rows; a_3 is the distance from the last column to the loaded edge and a_4 is the distance from the outer rows to the lateral edge of the timber member.

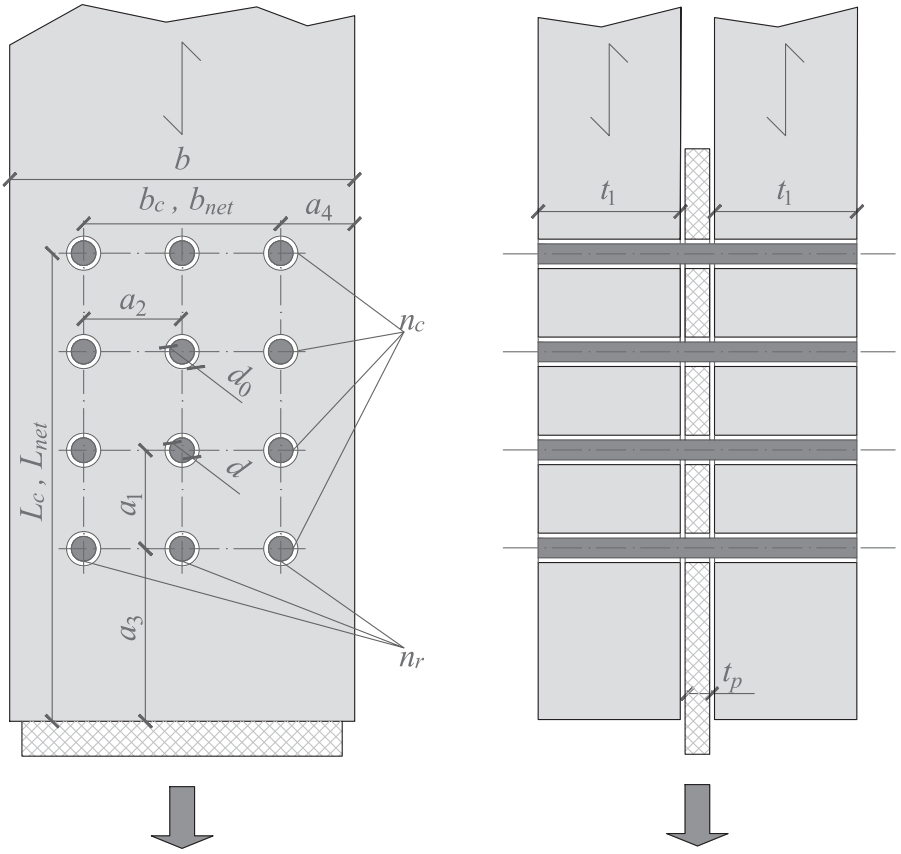

Fig. 2. Basic geometry of a generic timber-to-steel connection with large diameter fasteners.

The loaded timber area $b_c \times L_c$ (Fig. 2a) is defined from $b_c = a_2(n_r - 1)$ and $L_c = a_1(n_c - 1) + a_3$, and the corresponding net dimensions (which consider also the protruded holes of diameter d_0), are $b_{net} = b_c - [(n_r - 1)d_0]$, and $L_{net} = L_c - [(n_c - 0.5)d_0]$.

2.2. Failure modes of connections loaded parallel to the grain

From the possible failure modes of a timber connection loaded parallel-to-grain with large diameter fasteners shown in Fig. 1, only embedment (Fig. 1a) is a ductile failure mode, as considered by the European Yield Model (EYM). The other possible failure modes, all of them brittle, are:

- Splitting (Fig.1b): it is formed by a longitudinal crack along the row of fasteners. This failure might locally occur in the outer row, and the final global failure of a connection with multiple rows might not be related to it. It is, therefore, dismissed by authors such as Quenneville and Zarnani [9].
- Row shear (Fig. 1c): shear stresses generate two parallel cracks along each row of fasteners.
- Block shear (Fig. 1d): it is generated by the tear out of the loaded timber area, $b_c \times L_c$, defined by two lateral cracks along the exterior rows of fasteners and a head crack.
- Net tension (Fig. 1e): it is determined by a crack produced on the net cross sectional area at the beginning of the connection.

2.3. Existing brittle failure design models

Only three models consider somehow all the brittle failure modes in the parallel-to-grain direction: the Eurocode 5 [7], the model from Hanhijärvi and Kevarinmäki [10,11] and the one proposed by Quenneville and Zarnani [9]. However, as shown in previous works [12,5] they lack a consistent approach. A brief description of them is given below, and further details regarding the capacity of the involved failure planes will be described within Section 3. For a more detailed description and analysis, please refer to Yurrita and Cabrero [12].

Among the described brittle failure modes, the Eurocode 5 [7] only deals explicitly with block shear (Fig. 1d). The corresponding model is described in the informative Annex A, where the brittle capacity is obtained as the maximum of the capacities of the involved failure planes. Splitting (Fig. 1)b and row shear (Fig. 1c) are considered indirectly in the ductile calculation by introducing the factor n_{ef}. This value, derived from the work developed by Yurrita and Cabrero [13], reduces the ductile capacity of the connection by reducing the number of considered fasteners. Even though net tension failure is not explicitly considered for connections, it is said in Section 6.1.2 [7] that the wood members must withstand the loads (tension in this case) at any point of them, and this should be also accomplished in the connection.

Hanhijärvi and Kevarinmäki [10,11] also consider all the possible failure modes (including splitting) by a comprehensive calculation model which accounts for all the possible failure modes at once. The capacity of the timber element is obtained by adding the minimum of the brittle failure planes or the ductile mechanism. In consequence, the obtained capacity might not reflect the actual failure mechanism.

The model from Quenneville and Zarnani [9], which is the proposal for the future standard from New Zealand, is an upgrade of the model included in the Canadian code CSA Standard O86-09 [8], originally derived from the work from Quenneville and Mohammad [14], and Mohammad and Quenneville [15]. The capacity for each brittle failure mode is obtained by adding the corresponding capacities of the

involved failure planes. Only splitting is not considered, as it is not an expected failure mode in a connection with two or more rows of fasteners.

3. Considerations for the new design model

3.1. Considered failure planes

All the existing models are intended for design purposes, as the one herein presented. Hence, they aim at a simple model which is easy to understand by the designer. For that reason, the brittle capacity is obtained from the capacity of those planes where the failure may take place, and which are clear to the practitioner: the shear lateral planes *L* (related to row shear -Fig. 3a- and block shear -Fig. 3b-) and the head tension plane *H* (related to block shear -Fig. 3b- and net tension -Fig. 3c-). Such capacity is obtained by multiplying their area by the corresponding strength, either tensile parallel-to-grain $f_{t,0}$ or shear f_v. This section presents the different assumptions for the consideration of the capacity of these planes, discusses their adequacy and presents how they are considered in the new proposal.

3.1.1. Head tensile planes

All the models consider the net area for these tensile planes *H* (Fig. 3), as described below. No modifications are introduced in the proposal.

Head tensile plane for block shear. The area of the head tensile plane related to block shear $A_{T,b}$ is the net area comprised within the two lateral shear planes of the outer rows of fasteners, where the pre-drilled holes are not considered:

$$A_{T,b} = (a_2 - d_0)(n_r - 1)t \tag{1}$$

Head tensile plane for net tension.

The area of the head tensile plane (or net cross-section) related to net tension $A_{T,n}$ is the result of discounting the pre-drilled holes to the gross cross-sectional area of the timber element:

$$A_{T,n} = (b - d_0 n_r)t \tag{2}$$

3.1.2. Lateral shear planes

The existing models differ on how to consider these lateral planes *L*, which are activated in block shear (Fig. 3b, two planes) and in row shear (Fig. 3a, two planes per each row of fasteners). They assume different length and width, this latter related to the effective thickness of the timber member.

The number of considered lateral shear planes depends on the failure mode: two shear planes for block shear (Fig. 3b) or two shear planes per each row of fasteners in the case of row shear (Fig. 3a).

Length of lateral shear planes.

The models from Hanhijärvi and Kevarinmäki [10,11] and Eurocode 5 [7] consider the total length of the connection, $L_c = a_1(n_c - 1) + a_3$. On the other hand, Quenneville and Zarnani [9] propose a more conservative value, $L_c = n_c \min(a_1, a_3)$, obtained by multiplying the number of columns of fasteners by the minimum value between the parallel spacings, a_1 and a_3.

Experimental results suggest that considering the whole length of the connection might closer reflect the actual response. Fig. 4 shows two different connections tested by Yurrita et al. [12], in which the a_3 distance was the only difference between them: *LVLb3.a3* had $a_3 = 3d = 36$ mm (Fig. 4a, while *LVLb9.a3* had $a_3 = 9d = 108$ mm (Fig. 4c).

Fig. 4b and d show the load-slip behaviour of the performed tests. As a reference, the horizontal dashed line shows the theoretical load capacity, 159.20 kN, predicted by Quenneville and Zarnani [9]. It is the same for both configurations, because it is obtained from the minimum between a_1 and a_3, which in both cases is $a_1 = 36$ mm.

However, the test results show an increased capacity in those connections with higher end distance. The *LVLb3.a3* configuration reaches an average maximum load of 131.50 kN while the *LVLb9.a3* obtains a mean capacity of 191.68 kN, 45% higher. The difference of length between both configurations is around 35%, similar to the observed increase in load capacity.

It may be concluded that those models which consider the whole length of the lateral plane more closely reflect the actual behaviour of the connection. Therefore, the considered length of the connection in the new proposal is defined as $L_c = a_1(n_c - 1) + a_3$.

Width of the lateral planes: effective thickness.

The width of the lateral shear planes is usually defined by means of an effective thickness of the timber element, which allows for a simple way to consider the non-homogeneous stress distribution along the fastener and the resulting deformation.

The Eurocode 5 [7] bases its proposal in the yielding mechanism of the fastener. However, brittle failure may happen before yielding [16]. On the other hand, Quenneville and Zarnani [9] propose to determine the effective thickness based only on the position of the wood member in the connection: outer members can be found in wood-steel (*ws*, Fig. 5a), wood-steel-wood (*wsw*, Fig. 5b) and the exterior members of multiple shear plane (*msp*, Fig. 5d) connections. Inner timber members of a connection are used in steel-wood-steel (*sws*, Fig. 5c) connection and also as interior elements of *msp* joints. Depending on their relative position, they propose $t_{ef} = 0.65t$ and $t_{ef} = 1.0t$ for outer and inner timber members, respectively. Hanhijärvi and Kevarinmäki [10,11] also consider the relative position of the timber member, but additionally take into account geometrical and material properties of the fastener and the timber product.

In a previous study, Yurrita and Cabrero [16] analysed this parameter, and developed a new approach to determine it. The new proposal is based on the elastic deformation of the fastener, modelled by means of a beam-on-elastic-foundation. Only the slenderness t/d of the fastener (ratio between timber thickness t and fastener diameter d) is considered to be the main influencing parameter. The following expressions for thin ($t_p \leqslant 0.5d$) and thick ($t_p \geqslant 1.0d$) steel plates were developed by Yurrita and Cabrero [16]. The distinction made in the equations below between thin and thick steel plates is taken from the Eurocode 5 [7], which additionally suggests an interpolation of the obtained value for intermediate cases.

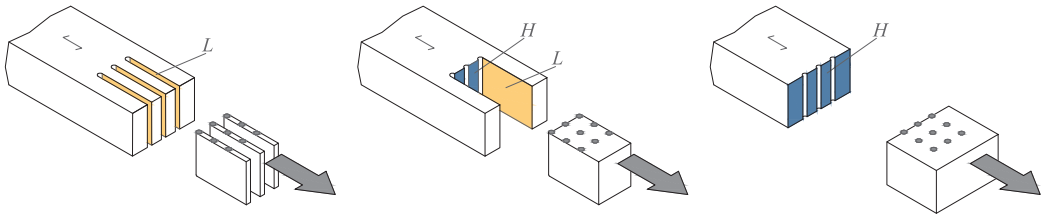

(a) Row shear (b) Block shear (c) Net tension

Fig. 3. Loading planes (lateral shear L, and head tensile H) related to each failure mode.

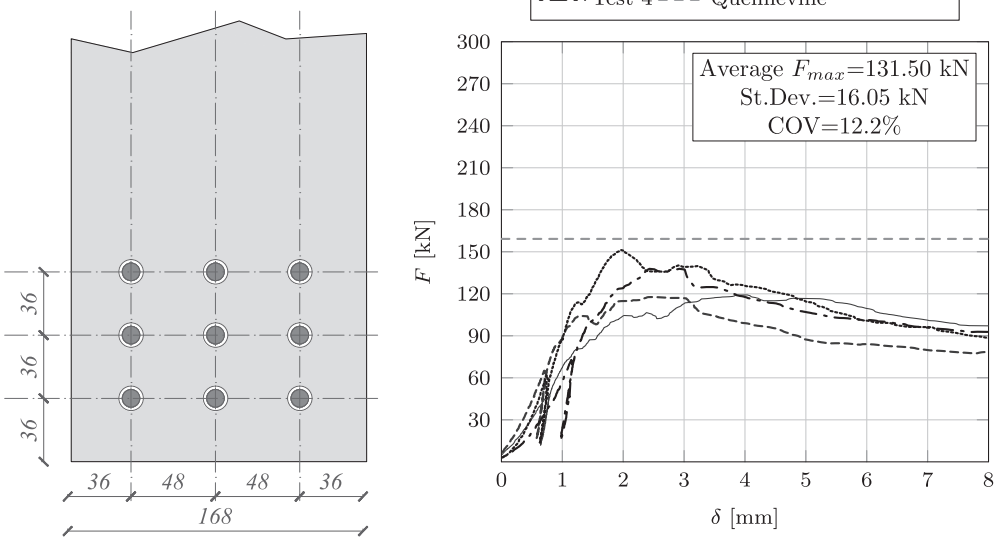

(a) *LVLb3.a3*: geometry (b) *LVLb3.a3*: test results

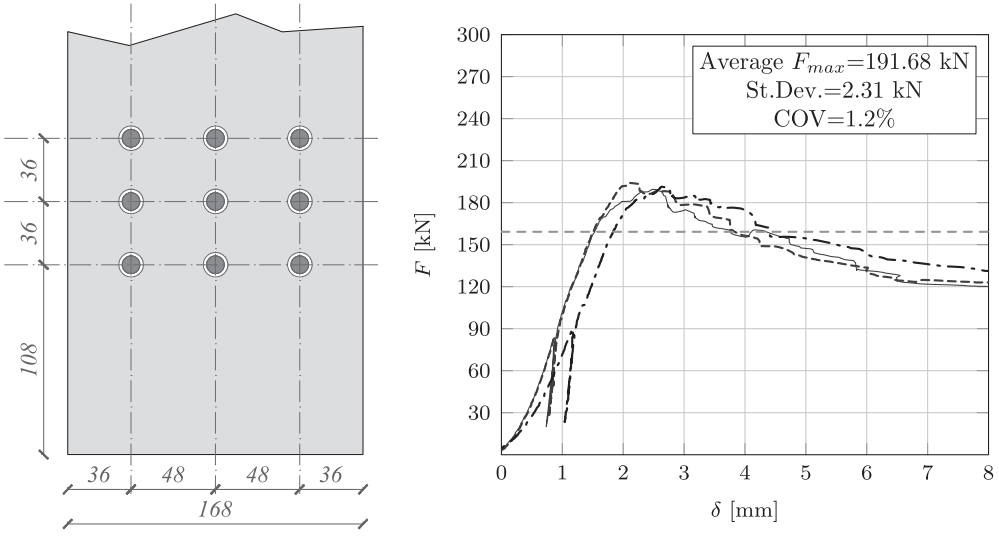

(c) *LVLb9.a3*: geometry (d) *LVLb9.a3*: test results

Fig. 4. Geometry and test results of the *LVLb3.a3* and *LVLb9.a3* test series performed by Yurrita et al. [12].

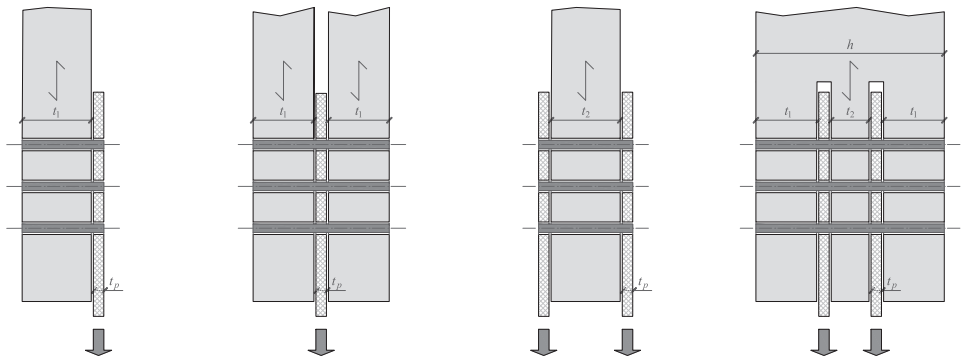

(a) ws side view (b) wsw side view (c) sws side view (d) msp side view

Fig. 5. Possible configurations of a timber connection combined with steel plates.

- Thin plates ($t_p \leqslant 0.5d$):

$$\text{Outer members:} \quad t_{ef} = \begin{cases} 0.66t & \text{if } \frac{t}{d} \leqslant 3 \\ \max\left(0.76 - \frac{t}{30d}; 0.2\right)t & \text{if } \frac{t}{d} > 3 \end{cases} \tag{3}$$

$$\text{Inner members:} \quad t_{ef} = \begin{cases} t & \text{if } \frac{t}{d} \leqslant 7 \\ \max\left(1.7 - \frac{t}{10d}; 0.5\right)t & \text{if } \frac{t}{d} > 7 \end{cases} \tag{4}$$

- Thick plates ($t_p \geqslant 1.0d$):

$$\text{Outer members:} \quad t_{ef} = \begin{cases} t & \text{if } \frac{t}{d} \leqslant 3 \\ \max\left(1.17 - \frac{t}{18d}; 0.35\right)t & \text{if } \frac{t}{d} > 3 \end{cases} \tag{5}$$

$$\text{Innermembers:} \quad t_{ef} = \begin{cases} t & \text{if } \frac{t}{d} \leqslant 11.5 \\ \max\left(1.95 - \frac{t}{12d}; 0.65\right)t & \text{if } \frac{t}{d} > 11.5 \end{cases} \tag{6}$$

3.2. Coefficients associated to each failure plane

All the existing models use numerical coefficients to modify the capacity of both failure planes. These parameters hide several assumptions which simplify the different complex phenomena involved in the connection behaviour, such as non-homogeneous stress distribution, stress interaction, or the probability of defects in the stressed timber volumes.

An overview of those different values is given in Table 1. The capacity of the lateral planes is reduced to around 70%, while that of the head tensile plane is increased.

The Eurocode 5 [7] and Quenneville and Zarnani [9] propose a fixed numerical value in both planes, while Hanhijärvi and Kevarinmäki [10,11] proposed different coefficients for different timber products.

Following this latter model, the proposal presents coefficients which are different for each timber product, and defined by the correspoding modulus of elasticity parallel-to-grain and the shear modulus (Table 1). This E_0/G ratio allows for a simple way to additionally consider the interaction between both types of stresses, as pointed out by Hanhijärvi and Kevarinmäki [11] and Sjödin and Johansson [17]. This approach will be validated below in Fig. 10 and the related discussion.

3.3. Determination of the brittle capacity from the failure planes

Once the capacity of the different failure planes is calculated, the total brittle capacity of the timber member must be obtained. Most of the proposals share the same principle, that is, the brittle capacity is obtained as the sum of the capacities of the involved planes. Only the Eurocode 5 [7] proposes a more conservative approach, in which the total load capacity is determined as the maximum between the capacity of the lateral shear planes and the head tensile plane. This latter procedure has been shown to be excessively conservative, and it is not related to the failure observed in the experimental tests [12]. Therefore, the new proposal proposes the addition of the capacities of the lateral shear and head tensile planes to obtain the brittle load capacity for block shear.

3.4. Considerations for the case of multiple shear planes connections

The models for brittle failure, including the new proposal, provide the load capacity per timber element of the connection. Most of the connections have one (wood-steel, Fig. 5a) or two shear planes, (wood-steel-wood, Fig. 5b, and steel-wood-steel,Fig. 5c). In these cases, the total load capacity of the connection will be the sum of those of the timber members which share the load (1 element in the cases of Fig. 5a and c, or 2 symmetrical members for Fig. 5b).

However, in practice, connections with multiple shear planes are also used (Fig. 5d shows an example of a connection with four shear planes). In these cases, the simple addition of the load capacity of each timber member might not be adequate, since different timber sections might be used, and they therefore might not be simultaneously loaded at the same rate. As previously explained by Yurrita and Cabrero [18], a stiffness-based model is more adequate. The total capacity of the connection F_b can be then obtained from the load capacities $F_{B,1}$ and $F_{B,2}$ of the outer and inner timber members, respectively:

$$F_B = \min \begin{cases} F_{B,1}\left(2 + n_2 \frac{t_2}{t_1}\right) \text{ failure of outer members,} \\ F_{B,2}\left(2\frac{t_1}{t_2} + n_2\right) \text{ failure of inner members;} \end{cases} \tag{7}$$

where t_1 and t_2 are the thickness of the outer and inner wood members of the connection, and n_2 is the number of inner timber members in the connection. This expression assumes that the two outer elements are equal, and same consideration is taken for connections with several inner members.

4. Summary of the new model proposal

4.1. Brittle capacity of the connection

The brittle load capacity F_B of a connection may be obtained by adding the load reached by each of the timber members which share the load:

- Connections with one or two equal timber members (one or two shear planes):

$$F_B = nF_{B,i} \tag{8}$$

where $F_{B,i}$ is the capacity of a timber element and n is the number of timber elements.

- Connections with more than two timber members (usually referred asmultiple shear planes):

Table 1
Comparison of the coefficients applied to the shear (k_v) and tensile stresses (k_t for block shear and $k_{t,net}$ for net tension) used by the existing models (Eurocode 5 -Annex A- [7], Quenneville and Zarnani [9] and Hanhijärvi and Kevarinmäki [10,11]) and the proposal.

Model	k_v	k_t	$k_{t,net}$	Block shear
Eurocode 5 -Annex A- [7]	0.7[a]	1.5	1	$\max\begin{cases}\text{shear}\\ \text{tension}\end{cases}$
Quenneville and Zarnani [9]	0.75	1.25	1	shear + tension
Hanhijärvi and Kevarinmäki [10,11]	$\begin{cases}1 \text{ for GL}\\ 0.7 \text{ for LVL}\end{cases}$	$\begin{cases}2 \text{ for GL}\\ 1.7 \text{ for LVL}\end{cases}$	1	shear + tension [b]
Proposal	$0.4 + 1.4\sqrt{\frac{G}{E_0}}$	$0.9 + 1.4\sqrt{\frac{G}{E_0}}$	1	shear + tension

[a] Row shear is not considered in Eurocode 5 -Annex A- [7], so this coefficient is only applied to block shear.

[b] This is just a simplification, as this model is more complex and considers more interactions.

$$F_B = \min \begin{cases} F_{B,1}\left(2 + n_2 \frac{t_2}{t_1}\right) \text{ failure of outer members,} \\ F_{B,2}\left(2\frac{t_1}{t_2} + n_2\right) \text{ failure of inner members;} \end{cases} \quad (7\ \textit{revisited}),$$

where $F_{B,1}$ and $F_{B,2}$ are the capacities of the outer and inner timber members, respectively and n_2 is the number of inner timber members.

4.2. Brittle load capacity of a timber member

The brittle capacity $F_{B,i}$ of a single timber element i is obtained as the minimum of the capacities for the different possible failure modes.

The row shear capacity of a timber member $F_{B,rs,i}$ is determined by adding the capacity $F_{L,i}$ of the two lateral shear failure planes generated by each row of fasteners:

$$F_{B,rs,i} = 2n_r F_{L,i} \quad (9)$$

where n_r is the number of rows and $F_{L,i}$ is the shear capacity of the lateral plane given in (11).

The block shear capacity $F_{B,bs,i}$ is defined by the onset of failure of two lateral shear planes and a head tensile plane, and it is therefore obtained by adding the corresponding capacities:

$$F_{B,bs,i} = 2F_{L,i} + F_{T,i} \quad (10)$$

where $F_{L,i}$ is the shear capacity of the lateral (longitudinal, L) shear plane given in (11) and $F_{T,i}$ is the tension capacity of the head (transverse, H) plane given in (12).

The net tension capacity of a timber member $F_{B,nt,i}$ is determined by the load capacity of the net cross sectional area of the timber element, and obtained from the capacity of the tensile plane of the net transverse section of the connection $F_{T,net,i}$ defined in (13).

4.3. Plane Capacities

4.3.1. Lateral shear plane, L

The capacity of a single lateral longitudinal plane L of the timber member i may be defined as:

$$F_{L,i} = k_v t_{ef} L_c f_v \quad (11)$$

where the shear factor is $k_v = 0.4 + 1.4\sqrt{\frac{G}{E_0}}$; L_c is the length of the shear plane defined as $L_c = a_1(n_c - 1) + a_3$. and t_{ef} is the effective thickness defined as:

- Thin plates ($t_p \leqslant 0.5d$):

Table 2
Summary of the tests used for the validation of brittle failure.

Author	Number of		Joint scheme						Fastener Type		Timber product				Fastener pattern		Failure mode	
	Config.	Tests	*sws*	*ws*[a]	*ww*[a]	*wsw*	*www*	*msp*[b]	Bolt	Dowel	Glulam	LVL	CLT	Solid	Reticular	Stagger	Ductile	Brittle
Brittle failure tests																		
Massé et al. [19][c]	5	15	5	-	-	-	-	-	-	5	5	-	-	-	5	-	1	4
Mischler [24]	73	249	-	-	-	-	-	73	0	73	70	3	-	-	17	56	15	58
Quenneville and Mohammad [14][c]	37	370	37	-	-	-	-	-	37	-	36	-	-	1	37	-	6	31
Mohammad and Quenneville [15][c]	13	130	-	1	-	12	-	-	13	-	13	-	-	-	13	-	-	13
Anderson [25][c]s	3	9	-	1	2	-	-	-	3	-	3	-	-	-	3	-	-	3
Dodson [20]	6	27	6	-	-	-	-	-	6	-	6	-	-	-	6	-	-	6
Reid [21][c]	4	40	4	-	-	-	-	-	-	4	4	-	-	-	4	-	-	4
Sjödin and Johansson [17]	6	30	-	-	-	6	-	-	-	6	6	-	-	-	6	-	-	6
Leivo et al. [29][d]	4	12	-	-	-	4	-	-	-	4	4	-	-	-	4	-	-	4
SP [30][d]	2	4	-	-	-	-	-	2	-	2	2	-	-	-	2	-	-	2
Kevarinmäki [31][d]	1	3	1	-	-	-	-	-	1	-	1	-	-	-	1	-	-	1
VTT [32][d]	1	3	-	-	-	-	-	1	-	1	1	-	-	-	1	-	-	1
Hanhijärvi and Kevarinmäki [33][e]	39	118	16	-	-	13	-	10	-	39	23	16	-	-	39	-	-	39
Legras [22][f]	3	18	3	-	-	-	-	-	3	-	-	-	-	3	3	-	-	3
Hübner [26][c]	3	15	-	-	-	3	-	-	-	3	-	-	-	3	3	-	3	-
Misconel et al. [27][c]	2	10	-	-	-	2	-	-	1	1	-	2	-	-	1	-	2	-
Ottenhaus et al. [23]	6	30	-	-	-	6	-	-	-	6	-	3	3	-	6	-	2	4
Yurrita et al. [12]	28	110	-	-	-	-	-	28	-	28	16	12		-	28	-	-	28
Total brittle tests	236	1193	72	2	2	46	0	114	64	172	190	36	3	7	179	56	29	207
%	-	-	30.5%	0.8%	0.8%	19.5%	0%	48.3%	27.1%	72.9%	80.5%	15.3%	1.3%	3%	75.8%	23.7%	12.3%	87.7%
Ductile failure tests																		
Ehlbeck and Werner [34]	45	146	-	-	-	-	45	-	-	45	-	-	-	45	45	-	45	-
Ehlbeck and Werner [35]	47	141	-	-	-	-	47	-	-	47	-	-	-	47	47	-	47	-
Jorissen [13][c]	8	121	-	-	-	-	8	-	8	-	-	-	-	8	8	-	8	-
Ballerini [36]	8	24	-	-	8	-	-	-	-	8	-	-	-	8	8	-	8	-
Total brittle + ductile tests	344	1625	72	2	10	46	100	114	72	272	190	36	3	115	287	56	137	207
%	-	-	20.9%	0.6%	2.9%	13.4%	29.1%	33.1%	20.9%	79.1%	55.2%	10.5%	0.9%	33.4%	83.4%	16.3%	39.8%	60.2%

[a] As there is only two configurations of *ww* and *ws*, they been gathered with the *wsw* configurations for the validation in Section 5.2.2
[b] All the multiple shear connections have 4 shear planes, except three configurations with 6 and one with 8 shear planes.
[c] Only the test with two or more rows of fastener have been considered.
[d] Part of the results gathered by Kevarinmäki [28].
[e] One configuration has been discarded as the properties of the timber were not provided.
[f] Only the tests assembled and tested at normal moisture conditions are included.

Outer members: $$t_{ef} = \begin{cases} 0.66t & \text{if } \frac{t}{d} \leqslant \\ \max\left(0.76 - \frac{t}{30d}; 0.2\right)t & \text{if } \frac{t}{d} > 3 \end{cases} \quad (3 \textit{ revisited})$$

Inner members: $$t_{ef} = \begin{cases} t & \text{if } \frac{t}{d} \leqslant 7 \\ \max\left(1.7 - \frac{t}{10d}; 0.5\right)t & \text{if } \frac{t}{d} > 7 \end{cases} \quad (4 \textit{ revisited})$$

- Thick plates ($t_p \geqslant 1.0d$):

Outer members: $$t_{ef} = \begin{cases} t & \text{if } \frac{t}{d} \leqslant 3 \\ \max\left(1.17 - \frac{t}{18d}; 0.35\right)t & \text{if } \frac{t}{d} > 3 \end{cases} \quad (5 \textit{ revisited})$$

Inner members: $$t_{ef} = \begin{cases} t & \text{if } \frac{t}{d} \leqslant 11.5 \\ \max\left(1.95 - \frac{t}{12d}; 0.65\right)t & \text{if } \frac{t}{d} > 11.5 \end{cases} \quad (6 \textit{ revisited})$$

In the case of multiple shear plane connections, same formulae may be used. However, as the influence of the adjacent parts is not considered in the original, a reduction factor of 0.85 of the obtained effective thickness is recommended [16].

4.3.2. Head tensile plane, H

The capacity of the head tensile plane $F_{T,i}$ of the timber member i may be obtained as:

$$F_{T,i} = k_t A_{T,b} f_{t,0} \quad (12)$$

where the tensile factor is $k_t = 0.9 + 1.4\sqrt{\frac{G}{E_0}}$ and $A_{T,b}$ is the net area of the head tensile plane defined as $A_{T,b} = (a_2 - d_0)(n_r - 1)t$.

4.3.3. Tensile plane for net tension

The capacity of the tensile plane for net tension $F_{T,nt,i}$ is defined as:

$$F_{T,net,i} = A_{T,n} f_{t,0} \quad (13)$$

where $A_{T,n}$ is the net tensile plane area defined as $A_{T,n} = (b - d_0 n_r)t$.

5. Validation of the proposed model

5.1. Tests database

A total of 22 sets of tests (18 dealing with brittle failure and 4 focused in ductile behaviour) have been gathered for the validation of the model: seven of them were performed in North America (Massé et al. [19], Quenneville and Mohammad [14], Mohammad and Quenneville [15], Dodson [20], Reid [21] and Legras [22]), two in New Zealand (Ottenhaus et al. [23] and Yurrita et al. [12]), and the rest in Europe (Mischler [24], Anderson [25], Sjödin and Johansson [17], Hübner

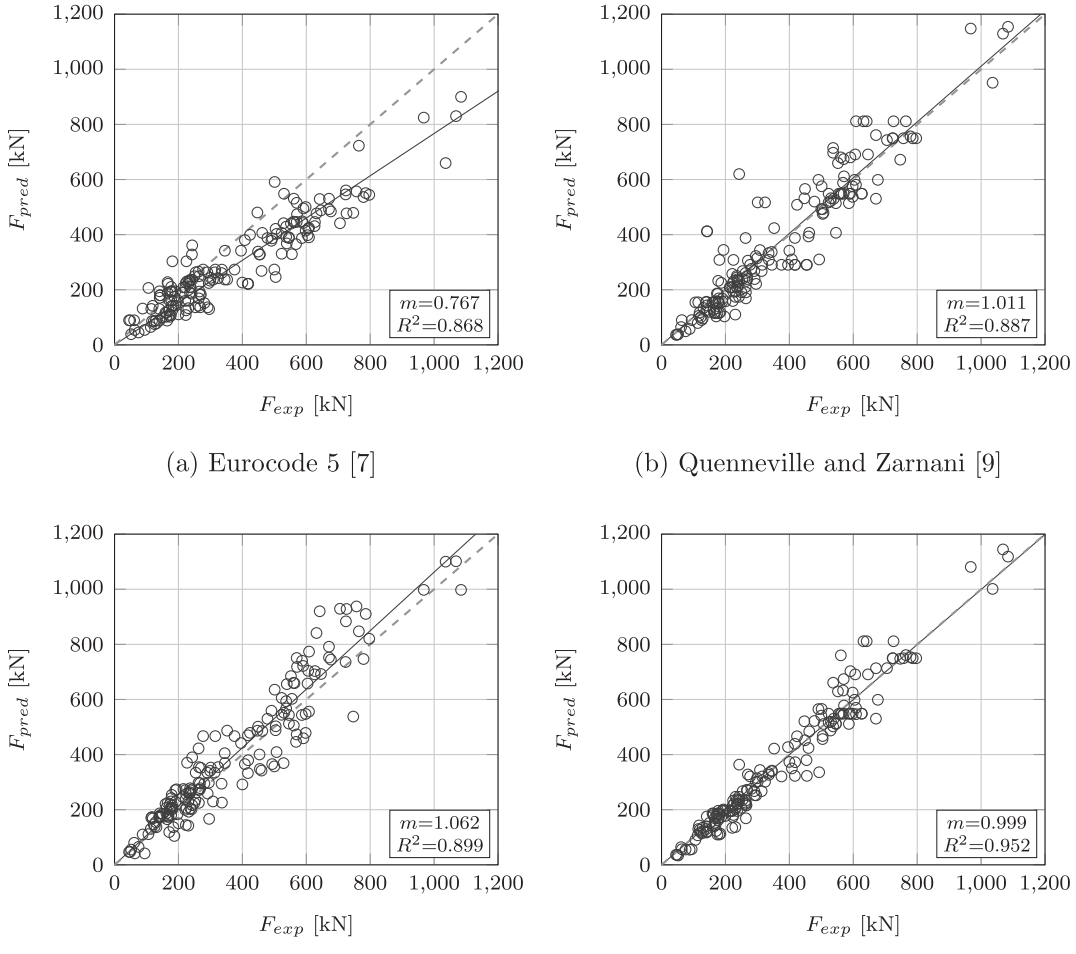

(a) Eurocode 5 [7]

(b) Quenneville and Zarnani [9]

(c) Hanhijärvi and Kevarinmäki [10, 11]

(d) Proposal

Fig. 6. Comparison between the load capacity values obtained from the tests F_T and the corresponding theoretical values F_P predicted by the models from Eurocode 5 [7], Quenneville and Zarnani [9], Hanhijärvi and Kevarinmäki [10,11], and. the proposal.

[26], Misconel et al. [27], the tests gathered in Kevarinmäki [28], which are the results of several reports performed by the VTT Technical Research Center of Finland –Leivo et al. [29], SP [30], Kevarinmäki [31], VTT [32] and Hanhijärvi and Kevarinmäki [33]–) and, finally, the ones focused on ductile failure (Ehlbeck and Werner [34,35], Jorissen [13] and Ballerini [36]).

A brief summary of the compiled tests is given in Table 2. Only those connections with two or more rows of fasteners have been included, as row shear and block shear are not expected to happen in connections with a single row of fasteners. In this latter case, splitting is the expected failure mode.

The validation process considers two different stages: first, an analysis of the accuracy of the brittle failure models to predict the brittle capacity (where only those research campaigns dealing with brittle failure are considered); second, assessment of the discrimination ability of each of the four models to determine whether a connection fails in a ductile or brittle manner (here also the tests failing in a ductile manner are considered).

At the first stage, after discarding some particular cases indicated in Table 2, a total of 1193 single tests distributed in 236 different configurations have been used for the validation. Three main joint schemes are the most represented: 30.5% of the configurations are steel-wood-steel (*sws*) connections, whereas 19.5% are wood-steel-wood (*wsw*) connections and the rest, 48.3%, are connections with multiple shear planes (*msp*), most of them with 4 shear planes (some with 6 and 8 shear planes). Two are the most represented types of fasteners, dowels (72.9%) and bolts (27.1%). Regarding the timber product, the most representative is glulam (80.5%), followed by LVL (15.3%) and with a symbolic presence of solid wood and CLT. Considering the fastener pattern, 75.8% were designed following a grid pattern, while the rest are staggered.

The former percentages vary considerably when considering the second stage, as most of the ductile tests were solid timber wood-wood-wood (*www*) connections. In this case, 344 configurations with a total of 1625 single tests were used. Brittle failure was reported in 60.2% of the tests, while the rest failed in a ductile way.

5.2. Comparison of the brittle failure accuracy of the models

The first part of the validation compares the test results of each configuration of the database that failed in a brittle way with the load capacity predicted by each of the three existing models (Eurocode 5 [7], Hanhijärvi and Kevarinmäki [10,11] and Quenneville and Zarnani [9]) and the proposal.

The small number of replicates for each configuration in the existing campaigns does not allow to obtain an accurate characteristic load and, hence, the validation is performed at the mean level. The required mean properties are obtained from the characteristic values following the procedure explained by Jockwer et al. [37] and Cabrero et al. [38] which is based on the probabilistic model for timber proposed by the Joint Committee on Structural Safety [39], and previously used in other works [5,18,12].

5.2.1. General analysis of the prediction accuracy

Fig. 6 provides an overview of the relation between the predicted theoretical values (ordinate axis) and the experimental ones (abscissa axis). The ideal correlation, 1: 1, is plotted as a dashed reference line. The figure includes a linear fitting passing through the origin of coordinates, and its corresponding slope m and correlation coefficient R^2.

A statistical analysis considering different metrics is additionally performed, and its results shown in Table 3. The different considered metrics are the coefficient of determination Q^2 [40,41] (best values are the closest to 1), the mean relative error *MRE*, and its corresponding standard deviation *SD* (lower values are the best ones), the slope m of the linear fitting (already given in Fig. 6), the correlation coefficient c [42] (values closer to 1 are the best) and the Concordance Correlation Coefficient *CCC* [43,41,44] (another time values closer to 1 are the best ones, with a recommended threshold value of 0.85). For a more detailed description, the reader is referred to Cabrero and Yurrita [5].

The Eurocode 5 [7] (Fig. 6a) is clearly the least accurate and most conservative model, with a slope $m = 0.767$. Moreover, it reaches consistently the worst results in all the metrics. On the opposite side, Hanhijärvi and Kevarinmäki [10,11] (Fig. 6c) tend to slightly overestimate the capacity of the connections ($m = 1.062$). The model from Quenneville and Zarnani [9] (Fig. 6b) obtains an almost ideal slope of $m = 1.011$. However, this model obtains a high dispersion of results, as demonstrated by parameters such as the correlation coefficient R^2 or the standard deviation *SD*. Both models can be considered to obtain quite similar results, as proved by the similar obtained *CCC*, which can be considered as a summary of the rest of the studied metrics.

Finally, the proposal (Fig. 6d) gets the best performance, since it commands all the metrics gathered in Table 3. It slightly improves the slope of Quenneville and Zarnani [9] in 1% and the R^2 from Hanhijärvi and Kevarinmäki [10,11] in 5%.

The boxplot from Fig. 7, which evaluates the ratio between the predicted F_{pred} and the tested capacity F_{exp}, summarizes the previous discussion. All the box (25th to 75th percentile of the results) from Eurocode 5 [7] falls below the ideal ratio $F_{pred}/F_{exp} = 1$. This additionally proves its conservative trend. The observed overestimation of results from Hanhijärvi and Kevarinmäki [10,11] can be clearly noticed; it additionally features almost no outliers, and all of them close the whiskers. Quenneville and Zarnani [9] has a more reduced box, which is located closer to 1 than the previous model but, in this case, several outliers are far from the whiskers (some of them even with a ratio close to $F_{pred}/F_{exp} = 3$). The proposed model shows the most reduced box and whiskers (least scatter), and both its median (depicted by the central line within the box) and average (cross inside the box) values are closer to the ideal ratio $F_{pred}/F_{exp} = 1$.

5.2.2. Detailed analysis of the involved parameters

An additional analysis is conducted by classifying the tests into three groups, according to the three most representative joint configurations in the database: steel-wood-steel (*sws*), wood-steel-wood (*wsw*), and multiple shear planes (*msp*). Fig. 8 plots this analysis in a similar way as previously done in Fig. 6. An ideal model should show the same slope $m = 1$ for the three joint configurations.

The proposal is the closest model to that ideal situation, with the three slopes ranging from 0.98 to 1.00, and a R^2 always higher than 0.89. The second best performance is reached by Quenneville and Zarnani [9] with slopes close to 1.00. However, this model obtains a low $R^2 = 0.65$

Table 3
Evaluation of the accuracy obtained by the four studied models: Quenneville and Zarnani [9] Eurocode 5 [7], Quenneville and Zarnani [9], Hanhijärvi and Kevarinmäki [10,11] and the proposal. The metrics used are the already used and described by Cabrero and Yurrita [5].

Model	Q^2	*MRE* (*SD*)	m	c	*CCC*
Eurocode 5 [7]	0.717	0.253 (0.199)	0.767	0.913	0.832
Quenneville and Zarnani [9]	0.864	0.154 (0.161)	1.011	0.930	0.938
Hanhijärvi and Kevarinmäki [10,11]	0.863	0.172 (0.144)	1.062	0.945	0.938
Proposal	**0.941**	**0.101 (0.102)**	**0.999**	**0.973**	**0.978**

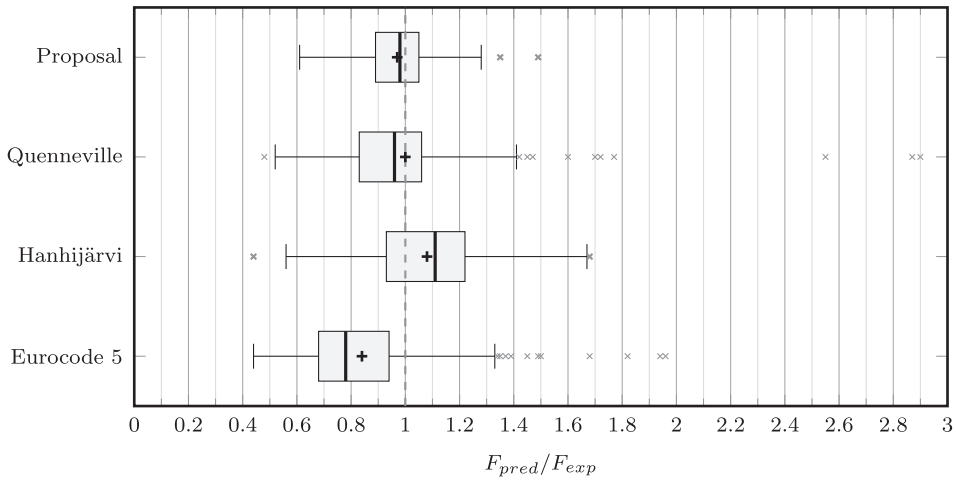

Fig. 7. Boxplot considering the accuracy of the predicted ratio between the predicted failure load F_{pref} and the tested failure load F_{exp}.

for the *wsw* connections, which is related to the determination of the effective thickness of the lateral plane, as will be seen later. In the case of Hanhijärvi and Kevarinmäki [10,11], it shows how it mainly overestimates those cases of *msp* joints (m = 1.108). Finally, the Eurocode 5 [7] gets different slopes for each joint configuration, and it is less conservative in the case of *wsw* connections.

Analysis of the influence of the fastener slenderness.

As the effective thickness of the timber member is one of the main

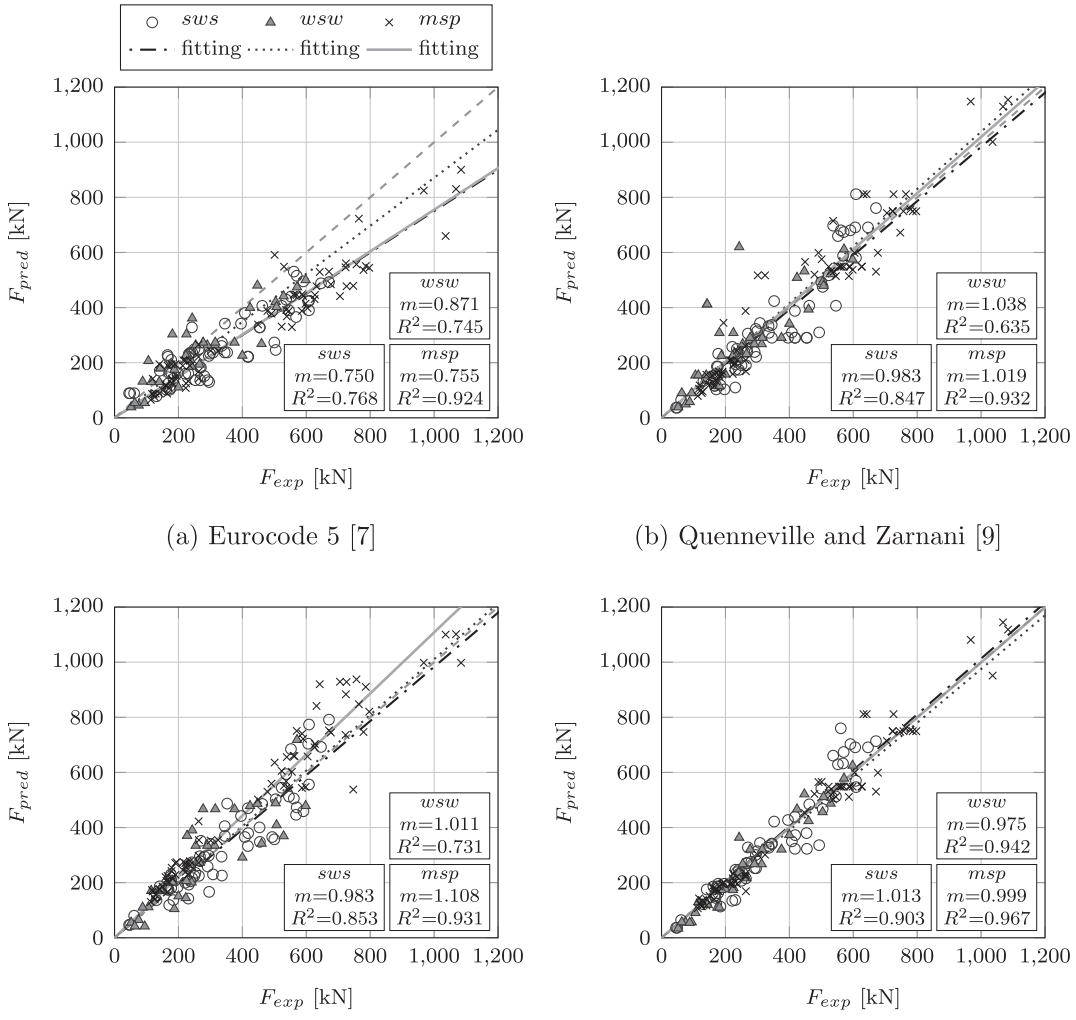

(a) Eurocode 5 [7]

(b) Quenneville and Zarnani [9]

(c) Hanhijärvi and Kevarinmäki [10, 11]

(d) Proposal

Fig. 8. Comparison between the values obtained from the tests and the corresponding theoretical values predicted by the models from Eurocode 5 [7], Quenneville and Zarnani [9], Hanhijärvi and Kevarinmäki [10,11], and the proposal. The results are divided by the joint configuration (*sws*, *wsw* or *msp*).

differences introduced in the new model, an analysis of its influence has been conducted, and its results are given in Fig. 9. The ratio F_{pred}/F_{exp} is given in the ordinate axis and the slenderness in the abscissa axis. The perfect correlation 1: 1 is plotted by a horizontal dashed line. The more horizontal and closer to 1 a fitting line is, the more accurate the predicted values are. In the case of the *msp* connections, the shown slenderness t/d for these cases is the average of those calculated for each of the timber elements.

The model from Quenneville and Zarnani [9] presents the most scattered graphic (Fig. 9b). Its results worsen as the slenderness increases, specially for the cases of *wsw*. The shown outliers in Fig. 7 correspond to cases with high slenderness, as already demonstrated by Yurrita and Cabrero [16]. The Eurocode 5 [7] also presents big differences among the different joint configurations, and it does not reach a horizontal slope for any case (Fig. 9a). The behaviour by Hanhijärvi and Kevarinmäki [10,11] (Fig. 9c) provides better general results, but again the best trend is achieved by the new model.

Analysis of the influence of the ratio E_0/G.

The new model proposes to define the associated coefficients to the tensile, k_t, and lateral planes, k_v, by means of the ratio between the modulus of elasticity parallel-to-grain E_0 and the shear modulus G of the timber product (see Table 1). The herein described analysis shows its suitability, according to the shown results in Fig. 10.

The two models which provide fixed values (Eurocode 5 [7] –Fig. 10a– and Quenneville and Zarnani [9] –Fig. 10b–) obtain the least consistent behaviour. In the case of Hanhijärvi and Kevarinmäki [10,11], who proposed different values depending on the timber product (Fig. 10c), there is a similar tendency for the three joint configurations: the average ratio F_{pred}/F_{exp} slightly decreases as the ratio E_0/G increases. The proposal (Fig. 10d) shows an improved accuracy. Therefore, establishing the coefficients k_v and k_t for the shear and tensile planes as a function of the ratio E_0/G seems to be the most adequate strategy.

5.3. Discrimination ability between brittle and ductile failure modes

The last stage of the validation process, as previously explained, evaluates the discrimination ability of each model to determine if a connection will fail in a brittle or ductile way. Such discrimination ability is plotted in Fig. 11, where the dark colours are related to the percentages of correct predictions (true ductile and true brittle) while the light ones depict those cases where the predictions were wrong (false ductile or false brittle).

The ductile capacity for both the model of Quenneville and Zarnani [9] and the new model corresponds to the EYM, but considering the actual number of fasteners, instead of the effective number of fasteners n_{ef}. In the case of the Eurocode 5 [7], two options are shown, as it does not explicitly provide the information of the failure mode when the n_{ef}

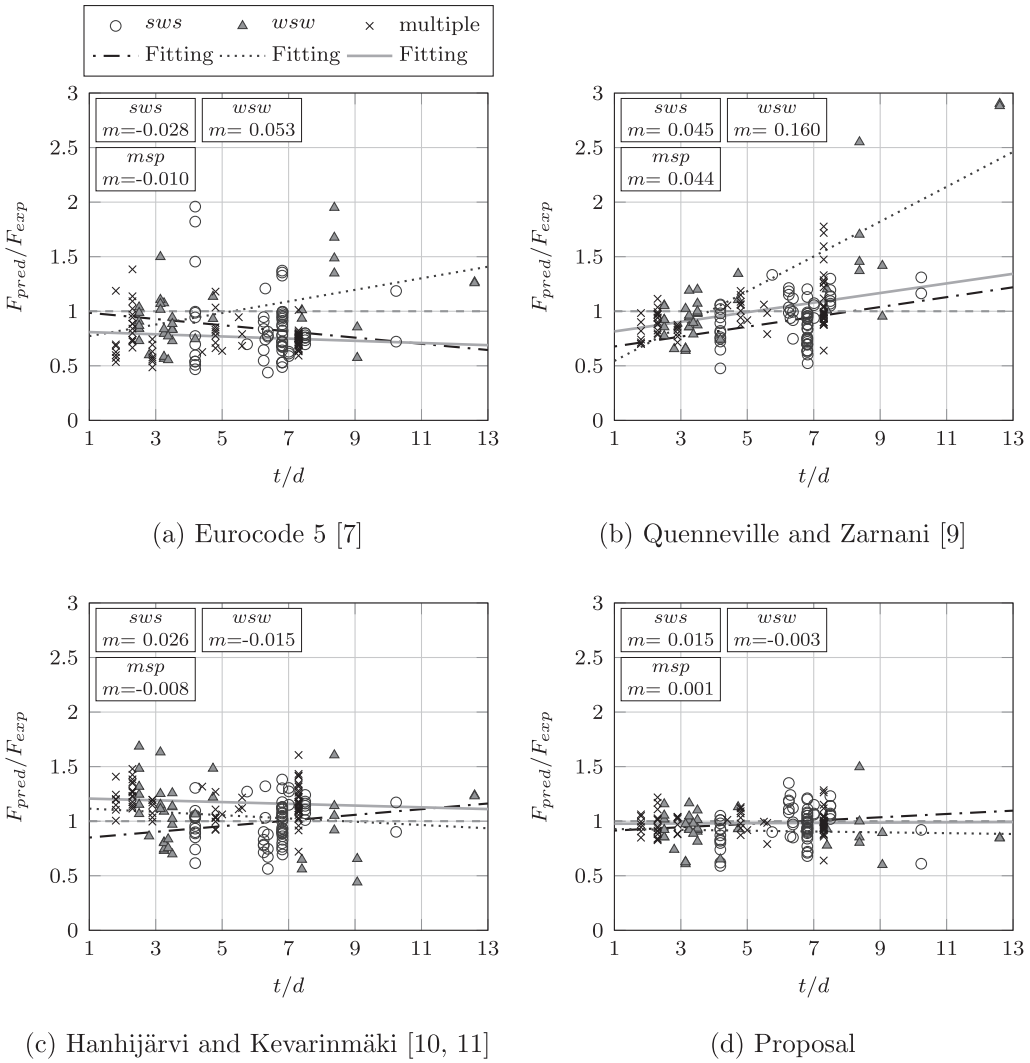

(a) Eurocode 5 [7]

(b) Quenneville and Zarnani [9]

(c) Hanhijärvi and Kevarinmäki [10, 11]

(d) Proposal

Fig. 9. Comparison of the prediction accuracy of the studied effective thickness approaches, combined with the model of Quenneville and Zarnani [9], considering the slenderness o.f the fasteners.

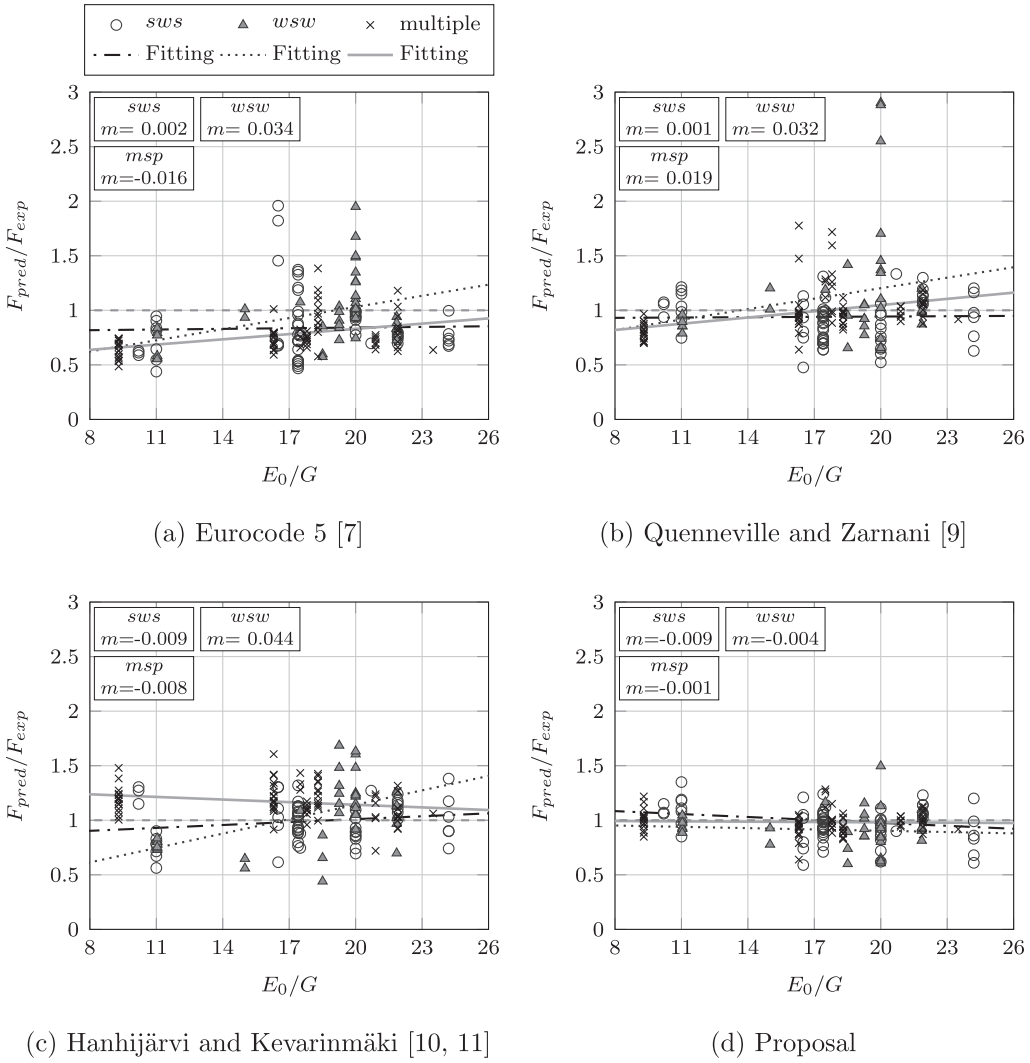

Fig. 10. Comparison of the prediction accuracy of the studied models, considering the stiffness ratio between the Modulus of elasticity parallel-to-grain E_0 and the shear modulus G..

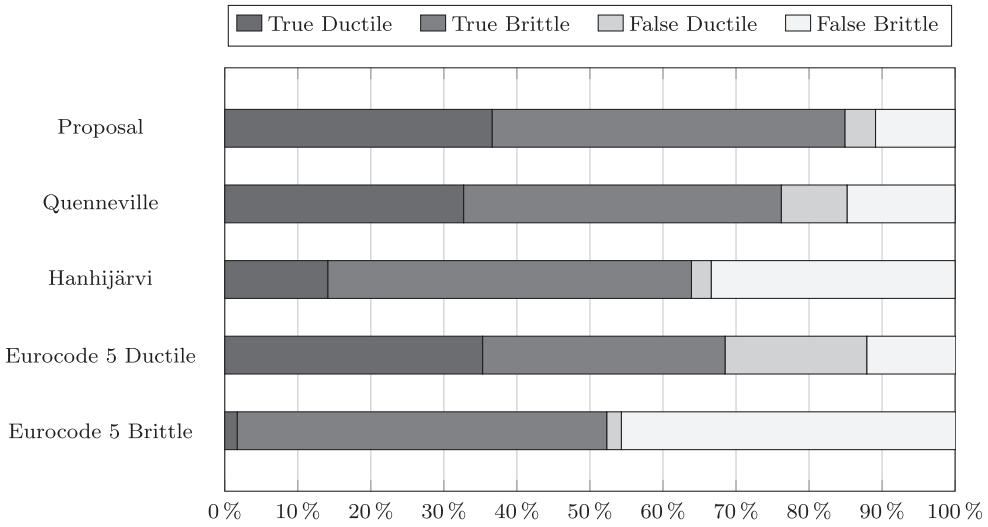

Fig. 11. Discrimination ability. Comparison between Eurocode 5 [7], Hanhijärvi and Kevarinmäki [10,11], Quenneville and Zarnani [9] a.nd the proposal.

is considered.

Therefore, the option named "Eurocode 5 Brittle", considers all the cases where n_{ef} is different from the actual n_c as brittle failure, whereas the second option ("Eurocode 5 Ductile") only considers brittle failure when the minimum capacity is that obtained by applying the Annex A model (therefore, all the cases where the minimum capacity

corresponds to the EYM with n_{ef} are considered to be ductile).

The best discrimination ability is achieved by the new model (85% of right predictions). The "brittle" option from Eurocode 5 [7] appears as the worst one, with only around 50% of true predictions. The "ductile" case, with almost 70% of correct failure modes, slightly improves the discrimination ability from Hanhijärvi and Kevarinmäki [10,11] (65%). The second position is for Quenneville and Zarnani [9] (around 75%).

6. Conclusions

A new model dealing with all the brittle failure modes for timber connections with large diameter fasteners is proposed. The new model tries to obtain a better prediction ability and, at same time, provides a calculation process with a limited complexity.

The new proposal takes the simplicity of the model from Quenneville and Zarnani [9] as a basis, and it additionally considers different assumptions. Some of the modifications include the effective thickness of the timber member, the length of the lateral shear planes, a different way to account for the interaction between shear and tensile stresses, or the special considerations for connections with multiple shear plane connections.

An extensive database of experimental results is used for the validation of the proposal, which is compared with the existing models. The model from the Eurocode 5 [7] can be considered as the worst one, as it tends to a clear underestimation of the load capacity of timber connections. Even if the model from Hanhijärvi and Kevarinmäki [10,11] obtains quite better results, it is a quite complex model. In both cases, it is not clear how to determine which is the predicted failure mode of the studied connection.

On the other hand, Quenneville and Zarnani [9] is a very simple and intuitive model. Regarding to its prediction accuracy, it reaches similar results than that from Hanhijärvi and Kevarinmäki [10,11], but it obtains a better discrimination ability between brittle and ductile failure modes.

The new proposal improves both the accuracy and discrimination ability of all the previous models, while being still quite a simple model to use and understand for practitioners. Therefore, it can be concluded that the new model improves all the existing models, reaching the best balance between accuracy and simplicity.

As a future work, a new model dealing with timber connections with small diameter fasteners (the ones which do not fully penetrate the whole timber thickness such as nails, screws or rivets) and plug-shear failure, similar to the one proposed herein, is required.

Declaration of Competing Interest

The authors declare that they have no known competing financial interests or personal relationships that could have appeared to influence the work reported in this paper.

Acknowledgements

The research has been performed thanks to the COST Action FP1402. The first author is supported by a PhD fellowship from the Programa de Becas FPU del Ministerio de Educación y Ciencia (Spain) under the Grant No. FPU15/03413. He would also like to thank the Asociación de Amigos of the University of Navarra for their help with a fellowship in early stages of this research. Finally, he would like to thank the Fundación Caja Navarra for supporting with a fellowship his stay in Auckland, New Zealand, where the first steps of this research were performed.

References

[1] Frühwald E, Serrano E, Toratti T, Emilsson A, Thelandersson S. Design of safe timber structures – How can we learn from structural failures in concrete, steel and timber? Design of safe timber structures – Report TVBK-3053. Tech. Rep. Lund University; 2007.
[2] Frühwald E. Analysis of structural failures in timber structures: Typical causes for failure and failure modes. Eng. Struct. 2011;33(11):2978–82. ISSN 01410296.
[3] Stepinac M, Cabrero JM, Ranasinghe K, Kleiber M. Proposal for reorganization of the connections chapter of Eurocode 5. Eng. Struct. 2018;170(May):135–45. https://doi.org/10.1016/j.engstruct.2018.05.058. ISSN 18737323.
[4] Fahlbusch H. Ein Beitrag zur Frage der Tragfaehigkeit von Bolzen in Holz bei statischer Belastung [Ph.D. thesis]. Technische Hochschule Braunschweig; 1949.
[5] Cabrero J, Yurrita M. Performance assessment of existing models to predict brittle failure modes of steel-to-timber connections loaded parallel-to-grain with dowel-type fasteners. Eng. Struct. 2018;171:895–910. https://doi.org/10.1016/j.engstruct.2018.03.037.
[6] Cabrero J, Yurrita M. State of the art report WG3 Design of connections in timber structures. Chap. A review of the existing models for brittle failure in connections loaded parallel to the grain, vol. 1. Germany: Technical University of Munich TUM; 2018b. p. 1979–83. iSBN 978-3-8440-6144-4.
[7] Eurocode 5, CEN:EN 1995-1-1:2004 - Eurocode 5: Design of timber structures - Part 1–1: General - Common rules and rules for buildings, Comité Européen de Normalisation (CTN); 2004.
[8] CSA Standard O86-09, Engineering design in wood. Canadian Standards Association; 2009.
[9] Quenneville P, Zarnani P. Proposal for the Connection Chapter of the New Zealand Design of Timber Structures; 2017 [Unpublished].
[10] Hanhijärvi A, Kevarinmäki A. Design method against timber failure mechanisms of dowelled steel-to-timber connections. In: CIB-W18 Timber Structures, Bled, Slovenia, Paper 40-7-3; 2007.
[11] Hanhijärvi A, Kevarinmäki A. VTT PUBLICATIONS 677: Timber Failure Mechanisms in High-Capacity Dowelled Connections of Timber to Steel, VTT, Espoo; 2008a. ISBN 9789513870904.
[12] Yurrita M, Cabrero JM, Quenneville P. Brittle failure in the parallel-to-grain direction of multiple shear softwood timber connections with slotted-in steel plates and dowel-type fasteners. Constr. Build. Mater. 2019;216:296–313. https://doi.org/10.1016/j.conbuildmat.2019.04.100.
[13] Jorissen AJ. Double shear timber connections with dowel type fasteners [Ph.D. thesis]. TU Delft; 1998.
[14] Quenneville P, Mohammad M. On the Failure Modes and Strength of Steel-Wood-Steel Bolted Timber Connections Loaded Parallel to Grain. Can. J. Civ. Eng. 2000;27(4):761–73.
[15] Mohammad M, Quenneville P. Bolted wood-steel and wood-steel-wood connections: verification of a new design approach. Can. J. Civ. Eng. 2001;28(2):254–63. https://doi.org/10.1139/l00-105. ISSN 0315–1468.
[16] Yurrita M, Cabrero JM. Effective thickness of dowel-type fasteners at the elastic range for steel-to-timber connections under brittle failure mode in the parallel-to-grain direction: a new method based on a beam on elastic foundation. Eng Struct XX; 2019. doi: 10.1016/j.engstruct.2019.109959 [in press].
[17] Sjödin J, Johansson C-J. Influence of initial moisture induced stresses in multiple steel-to-timber dowel joints. Holz als Roh- und Werkstoff 2007;65(1):71–7. https://doi.org/10.1007/s00107-006-0136-6. ISSN 0018–3768.
[18] Yurrita M, Cabrero JM. New criteria for the determination of the parallel-to-grain embedment strength of wood. Constr. Build. Mater. 2018;173:238–50. https://doi.org/10.1016/j.conbuildmat.2018.03.127.
[19] Massé D, Salinas J, Turnbull J. Lateral strength and stiffness of single and multiple bolts in glue laminated timber loaded parallel to grain. Tech. Rep. Ottawa, Canada: Engineering and Statistical Research Centre, Research Branch, Agriculture; 1998.
[20] Dodson MA. The Effects of Row Spacing and Bolt Spacing in 6-Bolt and 4-Bolt Wood-to-Steel Connections Master's thesis Washington State University; 2003.
[21] Reid MS. Predictions of Two-Row Multi-Bolted Connections Resistance Subjected to Parallel-to-Grain Loading [Master's thesis]. Ontario: Royal Military College of Canada; 2004.
[22] Legras BD. Effet de la teneur en humidité du bois sur la performance des assemblages bois boulonnés de pin gris, Master's thesis. Laval, Québec: Université; 2009.
[23] Ottenhaus L-M, Li M, Smith T, Quenneville P. Mode cross over and ductility of dowelled LVL and CLT connections under monotonic and cyclic loading, J Struct Eng 144(7). doi: 10.1061/(ASCE)ST.1943-541X.0002074.
[24] Mishler A. Bedeutung der Duktilität für das Tragverhalten von Stahl-Holz-Bolzenverbindungen [Ph.D. thesis]. ETH Zürich; 1998.
[25] Anderson GT. Experimental investigation of group action factor for bolted wood connections [Master's thesis]. Virginia Polytechnic Institute and State University; 2001.
[26] U. Hübner, Mechanische Kenngrößen von Buchen, Eschen und Robinienholz für lastabtragende Bauteile, Ph.D. thesis, Technische Universität Graz, 2013.
[27] M. Misconel, M. Ballerini, V. de Kuilen J W G, Steel-to-timber joints of beech-lvl with very high strength steel dowels, in: Proceedings of the World Conference on Timber Engineering, WCTE, Vienna, 269–276, ISBN 978-3-903024-35-9, 2016.
[28] A. Kevarinmäki, Design method for timber failure capacity of dowelled and bolted glulam connections. Research report number VTT-S-07046-09, Tech. Rep., VTT Technical Research Center of Finland, Helsinki, 2009.
[29] M. Leivo, V.M. Westman, M. Viinikainen, Teräslevyinen tappivaarnaliitos - liitoskokeet (Dowelled Steel-to-Timber Connection - Joint Tests), Tech. Rep., University of Applied Sciences, 2000.
[30] SP, Dragprovning av limträbalkar. Research report number SP 91B1. Ordered by Moelven Limträ A/S, Tech. Rep., Swedish National Testing and Research Intitute, 1992.
[31] A. Kevarinmäki, Ristipultilla vahvistetut puurakenteiden liitokset (Cross-bolt Reinforced Joints of Timber Structures). HUT/LSEBP Publication 64, Tech. Rep.,

Helsinki University of Technology, Helsinki, 1997.
[32] VTT, Monileikkeisten tappivaarnaliitosten kuormituskokeet (Loading Tests of Multiple Shear Dowelled Connections). Research report no RTE 1583/03. Ordered by Wood Focus Oy, Tech. Rep., Technical Research Center of Finland, 2003.
[33] A. Hanhijärvi, A. Kevarinmäki, Timber failure mechanisms in high-capacity dowelled connections of timber to steel. Experimental results and design. VTT Publications 677, Tech. Rep., Technical Research Center of Finland, 2008b.
[34] J. Ehlbeck, H. Werner, Tragfähigkeit von Laubholzverbindungen mit stabförmigen Verbindungsmitteln, Tech. Rep., Research report, Versuchsanstalt für Stahl, Holz und Steine, Karlsruhe University, 1989.
[35] J. Ehlbeck, H. Werner, Tragverhalten von Stabdübeln in Brettschichtholz und Vollholz verschiedener Holzarten bei unterschiedlichen Risslinienanordnungen, Tech. Rep., Research report, Versuchsanstalt für Stahl, Holz und Steine, Karlsruhe University, 1992.
[36] M. Ballerini, Experimental investigation on parallel-to-grain wood-to-wood joints with self-tapping screws, in: Proceedings of the World Conference on Timber Engineering, WCTE, Auckland New Zealand, 173–182, 2012.
[37] Jockwer R, Fink G, Köhler J. Assessment of the failure behaviour and reliability of timber connections with multiple dowel-type fasteners. Eng. Struct. 2018;172:76–84. https://doi.org/10.1016/j.engstruct.2018.05.081.
[38] Cabrero JM, Honfi D, Jockwer R, Yurrita M. A probabilistic study of brittle failure in dowel-type timber connections with steel plates loaded parallel to the grain. Wood Material Science & Engineering 2019;14(5):298–311. https://doi.org/10.1080/17480272.2019.1645206.
[39] Joint Committee on Structural Safety (Ed.), Probabilistic Model Code, JCSS, 2006.
[40] Steyerberg EW, Vickers AJ, Cook NR, Gerds T, Gonen M, Obuchowski N, Pencina MJ, Kattan MW. Assessing the Performance of Prediction Models. Epidemiology 2010;21(1):128–38. https://doi.org/10.1097/EDE.0b013e3181c30fb2. ISSN 1044–3983.
[41] Chirico N, Gramatica P. Real external predictivity of QSAR models: How to evaluate It? Comparison of different validation criteria and proposal of using the concordance correlation coefficient. J. Chem. Inf. Model. 2011;51(9):2320–35. https://doi.org/10.1021/ci200211n. ISSN 15499596.
[42] Alexander DL, Tropsha A, Winkler DA. Beware of R^2: Simple, Unambiguous Assessment of the Prediction Accuracy of QSAR and QSPR Models. J. Chem. Inf. Model. 2015;55(7):1316–22. https://doi.org/10.1021/acs.jcim.5b00206. ISSN 15205142.
[43] Gramatica P, Sangion A. A Historical Excursus on the Statistical Validation Parameters for QSAR Models: A Clarification Concerning Metrics and Terminology. J. Chem. Inf. Model. 2016;56(6):1127–31. https://doi.org/10.1021/acs.jcim.6b00088. ISSN 15205142.
[44] Chirico N, Gramatica P. Real external predictivity of QSAR models. Part 2. New intercomparable thresholds for different validation criteria and the need for scatter plot inspection. J. Chem. Inf. Model. 2012;52(8):2044–58. https://doi.org/10.1021/ci300084j. ISSN 15499596.